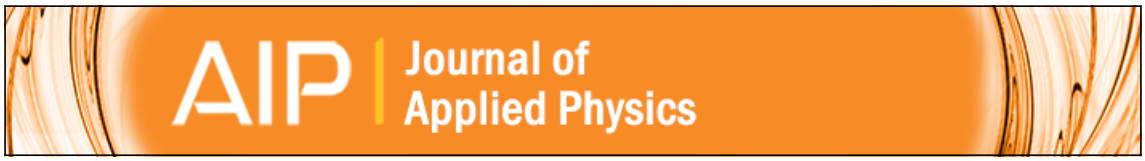

Spatially variable reaction in the formation of anodically grown porous silicon structures

O. Teschke, M. C. dos Santos, M. U. Kleinke, D. M. Soares, and D. S. Galvão

Citation: Journal of Applied Physics **78**, 590 (1995); doi: 10.1063/1.360577

View online: http://dx.doi.org/10.1063/1.360577

View Table of Contents: http://scitation.aip.org/content/aip/journal/jap/78/1?ver=pdfcov

Published by the AIP Publishing

Spatially variable reaction in the formation of anodically grown porous silicon structures

O. Teschke, M. C. dos Santos,[a] M. U. Kleinke, D. M. Soares, and D. S. Galvão
Instituto de Fìsica, Universidade Estadual de Campinas, 13081-970 Campinas SP, Brazil

(Received 30 June 1994; accepted for publication 14 March 1995)

In porous silicon formations there is an increase of dissolution rate at the fluorine-covered sites of the silicon surface due to the presence of excess electrons coming from oxidation of molecular hydrogen at the passivated (hydrogen-covered) sites. The dissolution rate increase in the presence of excess charge at the fluorine-covered sites is experimentally measured and a theoretical investigation is carried out by a semiempirical Hartree–Fock calculation. This spatially variable dissolution generates the porous silicon surface. © *1995 American Institute of Physics.*

The properties of visible room-temperature luminescence from anodically grown porous silicon (PS) have recently generated intense study.[1] Luminescence from PS passivated with oxygen rather than hydrogen[2] has ruled out SiH_x species, and the absence of Si–O bonding in IR-absorption data from PS[3] has ruled out siloxenes as luminescent species. A growing consensus has emerged for explaining the luminescence with quantum confined structures.[4,5] In spite of their degree of interest, the basic formation mechanisms[6] of porous silicon are, nevertheless, in dispute. Another noteworthy issue is that no matter how the silicon slabs are anodized, in some cases amounting to a few tens of volts, the formed porous structure is covered by hydrogen only.[3,7] Turner,[8] and subsequently Memming and Schwandt[6] and Unagami,[9] investigated the conditions of PS formation. Various analysis techniques have recently been recruited to study this system but the main features of PS growth still come from current versus voltage ($I-V$) experimental curves, and a basic knowledge of silicon electrochemistry is essential to understand the fundamentals of pore formation. In this paper, we report on current versus iR-free potential measurements, which suggest a mechanism for the dissolution process. The experimental results are interpreted based on electronic structure calculations on a model silicon cluster.

Single-crystal, polished silicon ⟨100⟩ and ⟨111⟩ oriented wafers (p and n types) of high and low resistivities were cut into rectangles with areas of approximately 1.0 cm^2. The etching bath was a 50:50 (by volume) solution of aqueous 48% HF (Merck) and 95% ethanol (Merck). The samples were etched galvanostatically with a model 273A potentiosat/galvanostat (Princeton Applied Research). The infrared spectrum obtained from ⟨100⟩ samples with $\rho=0.006\ \Omega$ cm, anodized with a current density of 20 mA/cm^2, showed bands characteristic of species like $-SiH_3$, $>SiH_2$, and $\rightarrow SiH$.[10] Similar curves were obtained for high-resistivity silicon samples. Both types of samples present mono-, di-, and trihydrogenated silicon atoms, indicating that the silicon surface is covered with hydrogen. The photoluminescence spectra of PS obtained under the polarization condition previously described[3,11] show broad photoluminescent bands.

The $I-V$ characteristics of p- and n-type silicon, both lightly and heavily doped, were measured. The electrodes were initially polarized at −4 V versus a saturated calomel electrode (SCE) for 5 min; increasing the voltage from −4 V vs SCE at a rate of 5 mV/s, one observes the full line in Fig. 1, in agreement with previously published $I-V$ curves.[12] A technique to remove the iR component from these data was used,[13] and the result is shown in Fig. 1 as the dot–dashed line. A prominent feature of this figure is that, although the silicon slab is being anodized in a 10 V applied voltage cell, the iR-corrected electrode potential value in the initial stage of porous silicon layer formation is approximately 0 V versus a standard hydrogen electrode (~ −250 mV vs SCE) for heavily doped p-type silicon. The silicon slab is anodized with hydrogen evolution and a Tafel slope of 60 mV/decade is measured. After anodizing the sample for 5 min at a current density of 50 mA/cm^2, the dashed line in Fig. 1 is obtained. A porous silicon layer is now observed at the electrode surface by its yellowish luminescence when illuminated with UV radiation. Our results show identically shaped current versus iR-free potential curves for highly doped n-type silicon. A similar behavior for lightly doped p and n types ($\geq$5 mA/cm^2) with the exception of a shift of a few hundred millivolts was also measured. This shift has been previously described and may be associated with voltage differences in the interfacial space charge.[1] Consequently, for a given rate of charge transport to the surface and hence a given rate of surface oxidation, the chemical aspects of dissolution are essentially the same for all silicon samples.

Though the detailed mechanism of silicon dissolution in HF is still not clear,[14] the porous surface is probably formed as follows: The surface is covered by hydrogen at the passivated sites and by fluorine at the active sites, the latter promoting silicon dissolution. Some H_2 is formed and may react with the nonpolar domains covered by hydrogen (F-covered sites have polar bonds and are supposed to interact with polar species like HF), injecting H^+ into the solution and transferring electrons to the silicon surface. These electrons could either go to the conduction band of bulk silicon or migrate to F-covered domains. The hydrogen presence at the solid/electrolyte interface plays a role in determining the potential of porous silicon formation. If the potential is increased to reach the etching polarization potential, a uniform silicon

[a]Electronic mail: cristina@ifi.unicamp.br

 0021-8979/95/78(1)/590/3/$6.00

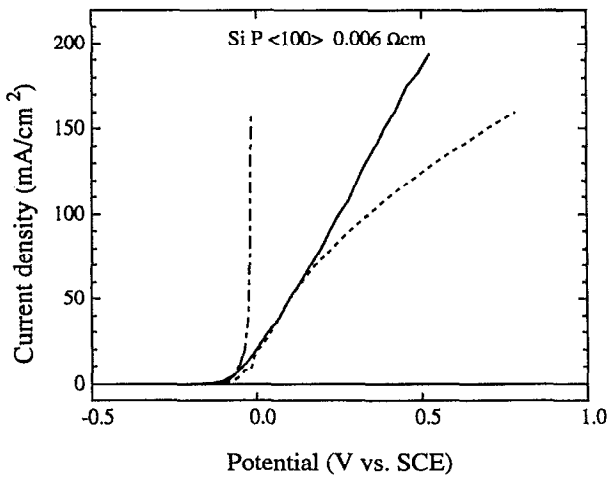

FIG. 1. Current–voltage characteristics of the silicon–hydrofluoric acid system measured by the current interruption method described in Ref. 13, on p-type (0.006 Ω cm), ⟨100⟩ oriented silicon samples. The full line (—) is the visual $I-V$ curve, while the dot–dashed (–·–) line corresponds to the IR-free current vs voltage data. Both curves were taken before the formation of a porous silicon layer. The dashed line (--) is the $I-V$ curve obtained after anodizing the sample for 5 min at a current density of 50 mA/cm^2. A yellowish luminescence is observed by illumination with UV radiation.

dissolution is observed. This comes as a consequence of total removal of surface hydrogen atoms and an irrestricted fluorine coverage.

In order to verify the silicon dissolution model, the following experiment was performed. The silicon electrode was polarized at low voltages around the equilibrium potential, resulting in low current densities. If hydrogen was bubbled on the silicon surface, the current increased and the electrode effective potential decreased following the load line imposed by solution resistance (see Fig. 2). When bubbling was interrupted the electrode potential increased to its original value. This was performed for various polarization voltages.

The dissolution mechanism has also been investigated at the molecular level by means of geometry optimizations on a silicon cluster (both neutral and with excess of negative charge). The calculations were carried out in the framework

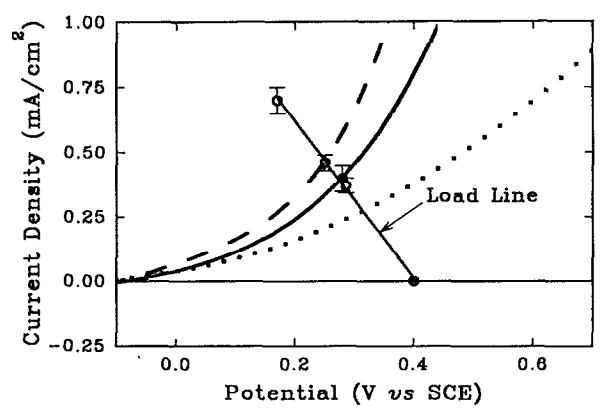

FIG. 2. Effect of hydrogen bubbling on the silicon surface: there is a current increase and an effective potential decrease following the load line imposed by solution resistance.

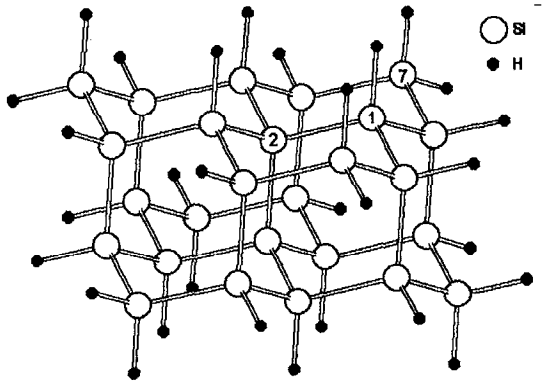

FIG. 3. Cluster of 26 silicon atoms adopted in the calculations. Atoms 1 and 7 are typical of ⟨111⟩ and ⟨100⟩ planes, respectively.

of the semiempirical Austin method 1.[15] The cluster adopted includes up to 26 silicon atoms and is shown in Fig. 3, with hydrogen saturation of the dangling bonds. Notice the presence of two different silicon terminations at the "surface": there are Si–H and Si–H_2 sites representing ⟨111⟩ and ⟨100⟩ orientations, respectively, which are the orientations of the samples used in our experiments. All bonding parameters (bond lengths, angles, and dihedrals) have been optimized.

Fluorine substitution at Si–H and Si–H_2 sites has been considered, since F^- (or HF_2^-) ion are attracted by the polarized electrode and start the corrosion reaction.[14] We have chosen atoms 1 and 7 shown in Fig. 3 to represent typical sites at ⟨111⟩ and ⟨100⟩ planes, respectively. Substitution at atom 7 leads to a cluster total heat of formation that is about 4 kcal lower (more stable) than the corresponding system substituted at atom 1, in agreement with the different corrosion rates measured for these directions.[14] In both cases, an increase in Si–Si bond lengths around the fluorinated site is observed, from 2.36 to 2.42 Å for atom 1 and 2.38 to 2.43 Å for atom 7. When electrons are added to the cluster, the extra charge results in larger stabilization of fluorinated clusters compared to the fully hydrogenated one (by 3 kcal), due to the polarization of Si–Si back bonds produced by the Si–F dipole at the surface. Electrons transferred from the H_2 oxidation reaction at the passivated domains are thus likely to migrate to the activated domains. A distribution of activated and passivated sites is thus formed on the electrode.

The dissolution process may involve the interaction of HF molecules with the active domains. The situation is now very different for atoms at ⟨111⟩ and ⟨100⟩ planes: attack of HF at the F-activated atom 1 leads to the breaking of a Si–Si bond, fluorination of atom 1, and hydrogenation of atom 2 (in the present model this is the best reaction representation on a real surface). Reaction equations and calculated enthalpies are

$$[Si_{25}H_{29}]{\equiv}Si{-}F+HF{\rightarrow}[Si_{25}H_{30}]{=}SiF_2,$$

$$\Delta H=-3.1 \text{ kcal}.$$

$$[Si_{25}H_{29}]{\equiv}Si{-}F+2e^-+HF{\rightarrow}\{[Si_{25}H_{30}]{=}SiF_2\}^{2-},$$

$$\Delta H=-40.9 \text{ kcal}.$$

A high activation energy could be anticipated for these reactions due to the breaking of a Si–Si bond.[16] Though exothermic, the entalpy of the first reaction is low as a consequence of a strong geometry relaxation. Modifications of the molecular geometry include the opening of the structure (a hole at the ⟨111⟩ surface) and the weakening of the $Si–SiF_2$ bonds, which are increased to 2.47 Å and can allow the separation of SiF_2 fragments from the surface. On the other hand, the energetics of HF attack at ⟨111⟩ sites evidences the strong influence of the presence of negative charge on the cluster, as demonstrated by the enthalpy of the second reaction.

At atom 7, fluorination proceeds by substitution of a hydrogen and formation of H_2, following the equations

$$[Si_{25}H_{28}]=SiHF+HF\rightarrow[Si_{25}H_{28}]=SiF_2+H_2,$$

$$\Delta H=-21.9 \text{ kcal},$$

$$[Si_{25}H_{28}]=SiHF+2e^-+HF\rightarrow\{[Si_{25}H_{28}]=SiF_2\}^{2-}+H_2,$$

$$\Delta H=-63.0 \text{ kcal}.$$

Therefore these reactions are thermodynamically more favorable than the ones previously discussed, and the excess negative charge has the effect of considerably increasing the amount of energy released. In this case, also, $Si–SiF_2$ bond lengths increase to 2.46 Å. The energy required to separate the fragment is calculated to be of the order of 19 kcal and its dependence on the extra charges is negligible, since only about 12% of the negative charge localizes on the fragment. Inclusion of the separation step in the above reactions results in a release of 3 (neutral cluster) and 44 kcal (charged cluster) of energy. The dangling bonds left after separation of SiF_2 allow F^- ions to react and continue the corrosion reaction, while SiF_2 should react in solution[14] to produce H_2. Alternatively, dissolution could follow another series of reactions in which SiF_2 does not separate from the surface. Since the bonds connecting the fragment to the surface have weakened as compared to usual Si–Si bonds, reactions with HF are expected to be highly exothermic.

This mechanism thus provides a spatially variable corrosion rate distribution, where the H-covered sites are passivated by the $H_2\rightarrow 2H^+ + 2e^-$ reaction, which locally lowers the electrode potential by electron transfer. At F-covered sites the reaction rate is increased by the migration of electrons from H-covered sites. These sites will readily dissolve and a new silicon atom is now in contact with the solution, forming a pore as a consequence of the continuous reaction. Highly conductive silicon substrates facilitate the electron transfer from H-covered sites and consequently a minor portion of these sites are converted into a fluorine coverage. The high current density at these sites favors the formation of deep pores. In contrast, poorly conducting silicon samples require larger reaction areas due to the lower current density imposed by the bulk resistivity. The larger number of active sites results in a distribution of shallow micropores.

In summary, we have investigated the role played by hydrogen molecules in the formation mechanism of anodically grown porous silicon. It is experimentally observed that electron transfer enhances corrosion rates, which is obtained by bubbling hydrogen at a polarized electrode. A mechanism is proposed based on the assumption of a distribution of domains at the silicon surface: the passivated sites containing Si–H bonds and the activated sites covered by Si–F bonds. H_2 reacts, transferring electrons to the nonpolar, passivated sites; these electrons then flow toward the active domains where there is an increase in the corrosion rate. This spatially variable corrosion rate is responsible for pore formation. Electronic structure calculations give support to this mechanism since enthalpies calculated for fluorine substitution at the surface are strongly influenced by the presence of excess electrons. A marked difference in the energetics of reactions involving sites at ⟨111⟩ and ⟨100⟩ planes is found, in agreement with experimentally measured rates of corrosion for these directions.[17]

This work has been supported in part by the Brazilian Agencies FAPESP, FINEP, and CNPq.

[1] R. L. Smith and S. D. Collins, J. Appl. Phys. **71**, R1 (1992).
[2] V. Petrova-Koch, T. Muschik, A. Kux, B. K. Meyer, and F. Koch, Appl. Phys. Lett. **61**, 943 (1992).
[3] O. Teschke, Appl. Phys. Lett. **64**, 1986 (1994).
[4] L. T. Caham, Appl. Phys. Lett. **57**, 1046 (1990).
[5] V. Lehmann and U. Gosele, Appl. Phys. Lett. **58**, 856 (1991).
[6] R. Memming and G. Schwandt, Surf. Sci. **4**, 109 (1966).
[7] Y. Kato, T. Ito, and A. Hiraki, Jpn. J. Appl. Phys. **27**, L1406 (1988).
[8] D. R. Turner, J. Electrochem. Soc. **105**, 403 (1958).
[9] T. Unagami, J. Electrochem. Soc. **127**, 476 (1980).
[10] O. Teschke, F. Galembeck, M. C. Gonçalves, and C. U. Davanzo, Appl. Phys. Lett. **64**, 3590 (1994).
[11] L. R. Tessler, F. Alvarez, and O. Teschke, Appl. Phys. Lett. **62**, 2381 (1993).
[12] V. Lehman and H. Foll, J. Electrochem. Soc. **137**, 653 (1990).
[13] D. M. Soares, O. Teschke, and I. Torriani, J. Electrochem. Soc. **139**, 98 (1992).
[14] C. Levy-Clement, A. Lagoubi, R. Tenne, and M. Newmann-Spallart, Electrochim. Acta **37**, 877 (1992).
[15] M. J. Dewar, E. G. Zoebisch, E. F. Healy, and J. J. P. Stewart, J. Am. Chem. Soc. **107**, 4433 (1985).
[16] G. S. Higashi, Y. J. Chabal, G. W. Trucks, and K. Raghavachari, Appl. Phys. Lett. **56**, 656 (1990).
[17] D. B. Lee, J. Appl. Phys. **40**, 4569 (1969).